EFFECT OF BERYLLIUM HEAT TREATMENT IN SYNTHETIC RUBY

N. Monarumit [1], T. Lhuaamporn [2], S. Satitkune [1], W. Wongkokua [1*]

[1] Kasetsart University, 50 Ngam Wong Wan Rd., Chatuchak, Bangkok, 10900, Thailand; e-mail: wiwat.w@ku.ac.th
[2] The Gem and Jewelry Institute of Thailand, 140 ITF-Tower Building Silom Rd., Bangrak, Bangkok, 10500, Thailand

We study the effect of Be atoms in the corundum structure by using UV-Vis-NIR spectroscopy as well as X-ray absorption spectroscopy on synthetic ruby samples obtained by the Verneuil process. From the X-ray absorption near edge structure (XANES) spectra, the Be atoms are shown not to be related to the Cr environment. Furthermore, the UV-Vis-NIR absorption spectra are similar for the unheated, traditionally heated, and Be-heated synthetic ruby samples. However, the Be atoms are able to produce a brown-colored center, and the mixing of the red and the brown colors yields the orange in the Be-heated synthetic ruby samples. We propose that the orange color in the Be-heated synthetic ruby samples is caused by the Be^{2+} donor state at 475 nm (2.61 eV) in multiple UV-Vis-NIR wavelength excitation spectra.

Keywords: *synthetic ruby, beryllium, UV-Vis-NIR spectra, laser ablation inductively coupled plasma mass spectrometry, Cr K-edge X-ray absorption near edge structure spectra.*

ВЛИЯНИЕ БЕРИЛЛИЯ ПРИ ТЕРМООБРАБОТКЕ СИНТЕТИЧЕСКОГО РУБИНА

N. Monarumit [1], T. Lhuaamporn [2], S. Satitkune [1], W. Wongkokua [1*]

УДК 535.34:546.45

[1] Университет Касетсарт, Бангкок, 10900, Таиланд; e-mail: wiwat.w@ku.ac.th
[2] Таиландский институт драгоценных камней и ювелирных изделий, Бангкок, 10500, Таиланд

(Поступила 1 июня 2018)

С помощью спектроскопии в УФ, видимом и ближнем ИК диапазонах, а также рентгеновской абсорбционной спектроскопии исследовано влияние атомов бериллия на образцы синтетического рубина, полученные методом Вернейля. Из спектров рентгеновского поглощения вблизи краевой структуры (XANES) видно, что атомы Be не связаны с окружением Cr. Спектры поглощения в УФ-видимой-ИК (UV-Vis-NIR) области, полученные для ненагретых, традиционно нагретых и Be-термообработанных образцов синтетического рубина, похожи. Однако атомы Be способны образовывать коричневые центры, а смесь красного и коричневого цветов дает оранжевую окраску образцов синтетического рубина с нагретым Be. Предположено, что оранжевый цвет в образцах синтетического рубина с термообработанным Be обусловлен донорным состоянием Be^{2+} на 475 нм (2.61 эВ) в спектрах возбуждения в UV-Vis-NIR области.

Ключевые слова: *синтетический рубин, бериллий, спектры в УФ-видимом-ближнем ИК диапазонах, масс-спектрометрия с идуктивно-связанной плазмой с лазерной абляцией, краевая структура рентгеновских K-спектров поглощения Cr.*

Introduction. Ruby is a variety of the mineral corundum (α-Al_2O_3) that is mainly composed of Al_2O_3 with a chromium (Cr^{3+}) impurity. The color in ruby is caused by Cr^{3+} substituting for Al^{3+} in the corundum structure [1–3]. The beryllium (Be) heat treatment has been used as a new technique by many researches to describe the effect of Be in the corundum structure [4–14]. For example, orange sapphires have been obtained from Be-treated corundum with a high Cr content [8]. However, there are still no clear scientific descriptions that explain this physical effect.

It has been stated that the orange color in Be-treated pink sapphires is created by orange-colored centers [8]. In addition, blue sapphires can become yellow by Be heat treatment in an oxygen environment. The Be has been interpreted as being a catalyst in the heating process [9]. Furthermore, yellow or brown coloration of Be-treated synthetic sapphires has been achieved from the combination of $BeTiO_3$ clusters and Fe in the corundum structure [10–12]. The local environment of the trace elements in Be-treated sapphires was not influenced by the Be atoms, which was confirmed by Fe *K*-edge X-ray absorption near edge structure (XANES) spectra [13] as well as Cr *K*-edge XANES spectra [14]. Recently, Be atoms have been proposed to be active only in heat treatment in an oxygen environment to create a Be-trapped hole color center,which results in the yellow color of Be-treated sapphires [15].

In this study, we selected a synthetic ruby produced by the Verneuil process because the concentration of doped impurities can be assigned [16]. To investigate the effect of Be atoms in the corundum structure after heat treatment, we used multiple UV-Vis-NIR wavelength excitation spectroscopy, which involves multiple UV-Vis-NIR excitation wavelengths to probe the materials [17]. Furthermore, the data, including the chemical composition, the UV-Vis-NIR absorption spectra, CIELAB color indices and the UV fluorescence properties, were used to describe the cause of the color changes after heat treatment with Be. Moreover, the Be atoms have previously been proposed to be located in the environment of Cr^{3+} ions [18], which conflicts with another study [14]. Therefore, we obtained the Cr *K*-edge XANES spectra of the samples to verify its local environment.

Experimental. The synthetic ruby (SR) samples were collected with different Cr contents from a gem market. The samples were labelled as SR 1 and SR 2, and represented Cr contents of approximately 3000 and 6000 mg/kg, respectively, which were determined by laser ablation inductively coupled plasma mass spectrometry (LA-ICP-MS). Each sample was cut and polished perpendicular to the c-axis into three pieces: one piece was stored as the reference sample and the others were either traditionally or Be-heated, as shown in Fig. 1.

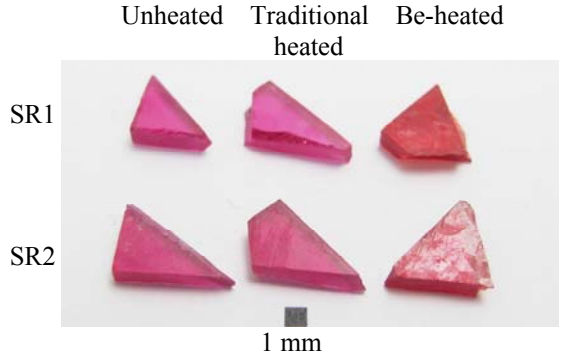

Fig. 1. Synthetic ruby prepared samples.

The heating experiments were divided into two groups. The first was a traditional heating at 1650°C in an oxygen environment without chemical addition and the second was the heating with Be, which was performed by a gem-trader using an electric furnace.

The chemical analysis using LA-ICP-MS, which is composed of laser ablation (New wave UP-213 model) and ICP-MS (Agilent 7500cs model), was performed to compare the concentrations of trace elements, such as Be, Cr and Fe, between the unheated and heated ruby samples. The reference standard material was NIST glass 610.

X-ray absorption spectroscopy (XAS) measurements of the synthetic ruby samples focused on the Cr *K*-edge with the XANES technique in fluorescence mode. XANES spectra were obtained at the XAS Beam line station (BL-8), located at the Synchrotron Light Research Institute (SLRI), Thailand, which employed the synchrotron radiation beam from eight bending magnets [19]. This measurement was set to detect the spectra at the Cr *K*-edge, which was related to a binding energy of approximately 5989 eV, using the Ge (220) double crystal monochromator with an energy resolution of 0.1 to 0.3 meV that was dependent on the width of the entrance slit. The specific parameters of this measurement were from 5969 to 6069 eV with a 0.2 eV energy step width and 1 s detection time using a 13-element Ge detector to obtain the spectra after four scans.

Each UV-Vis-NIR absorption spectrum of the samples was obtained to distinguish how the coloration was affected by the various heating conditions. UV-Vis-NIR spectroscopy was carried out using a Perkin Elmer UV-Vis-NIR spectrometer (Lambda^{TM} 900 model). Furthermore, multiple UV-Vis-NIR wavelength excitation spectra of the synthetic ruby samples were obtained in reflectance mode using a portable spectrometer with an integrating sphere. The colors of the samples were then identified using CIELAB indices. Moreover, the UV fluorescence properties of each sample were observed using a UV light box.

Results and discussion. The chemical concentration of the synthetic ruby samples is reported in Table 1. The Be, Cr, and Fe contents were compared among the unheated, traditionally heated, and Be-heated samples. The Be content clearly increased in the Be-heated synthetic ruby samples.

TABLE 1. Chemical Concentrations (mg/kg) with Standard Uncertainties of Be, Cr, and Fe in Synthetic Ruby Samples

Sample	Be	Cr	Fe
SR 1 (unheated)	0.92± 0.37	$(3.94 \pm 0.20)\times10^3$	15.6 ±6.4
SR 1 (traditionally heated)	1.19±0.52	$(3.54 \pm 0.18)\times10^3$	19.0 ±8.4
SR 1 (Be-heated)	15.6 ±1.3	$(3.83 \pm 0.19)\times10^3$	57.7 ±9.2
SR 2 (unheated)	0.96 ± 0.38	$(6.64 \pm 0.31)\times10^3$	12.2 ± 6.2
SR 2 (traditionally heated)	0.98 ± 0.43	$(6.31 \pm 0.30)\times10^3$	16.5 ± 7.1
SR 2 (Be-heated)	15.7 ± 1.3	$(6.39 \pm 0.31)\times10^3$	18.7 ± 7.8

Figure 2 shows the Cr *K*-edge XANES spectra of the unheated, traditionally heated, and Be-heated samples, which were plotted to show photon energy against normalized absorption (Xμ(*E*)) using the Athena program [20]. The spectral line shapes, as well as the peak positions, were distinctly similar for either the SR 1 or SR 2 samples. The pre-edge position and the absorption edge position of the samples showed the Cr^{3+}oxidation state for both the traditionally heated and Be-heated samples.

Table 2 shows the data analysis of the energy peak positions and the standard deviation of the synthetic ruby samples under different conditions. The values of the pre-edge and absorption edge peak positions (1 and 2) associated with its standard deviation, which were derived from the first derivative calculation, were not significantly different. The other positions, known as the post-edge positions (3, 4, and 5), were caused by the multiple scattering signal and were not related to the Cr oxidation state. Thus, the Be atoms were not located in the Cr environment.

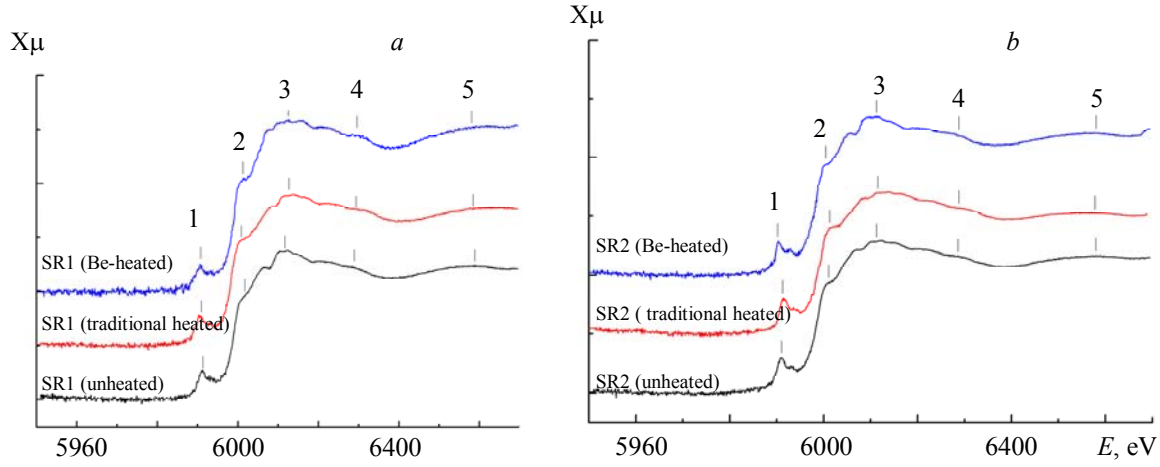

Fig. 2. Cr*K*-edge XANES spectra of synthetic ruby samples with different heat treatments for Cr contents of 3000 (a) and 6000 ppm (b).

TABLE 2. Energy Peak Positions and Standard Deviation of the Synthetic Ruby Samples

Samples	Pre-edge position 1 (eV)	Edge position 2 (eV)
SR 1 (unheated)	5991.0±0.2	6001.2±0.1
SR 1 (traditionally-heated)	5990.7±0.3	6001.3±0.1
SR 1 (Be-heated)	5990.6±0.4	6001.5±0.1
SR 2 (unheated)	5990.9±0.2	6001.2±0.1
SR 2 (traditionally-heated)	5990.7±0.2	6001.3±0.2
SR 2 (Be-heated)	5990.6±0.3	6001.3±0.2

Figures 3 and 4 show the comparison of the UV-Vis-NIR absorption spectra and the multiple UV-Vis-NIR wavelength excitation spectra of the synthetic ruby samples based on the different Cr concentration samples, SR 1 and SR 2. The UV-Vis-NIR absorption spectra of the synthetic ruby samples produced in the different conditions showed Cr^{3+} absorption peaks at 405, 555, and 693 nm. However, the pattern from the Be-heated samples exhibited a slightly wider absorption edge than the others. The spectrum showed a merging of two parts, that is, the red color and the brown color center, which were affected by the Be heat treatment [14]. Therefore, the Be-heated synthetic ruby sample that turned from red to orange was caused by the mixing between the red color of the ruby and the brown color center.

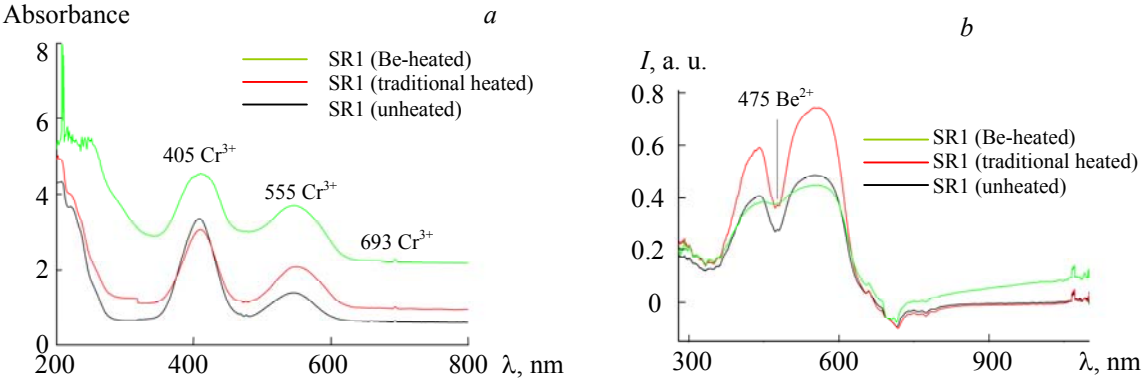

Fig. 3. Comparison of UV-Vis-NIR spectra (a) and multiple UV-Vis-NIR wavelength excitation spectra (b) of the synthetic ruby SR 1.

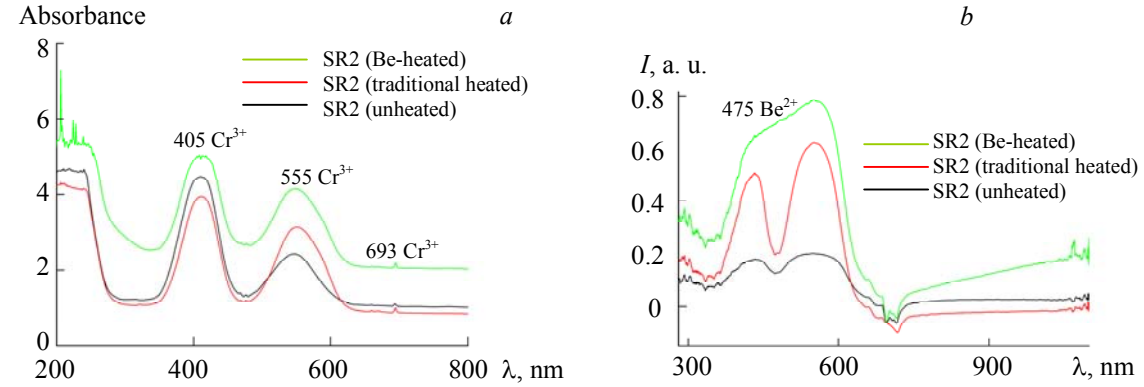

Fig. 4. Comparison of UV-Vis-NIR spectra (a) and multiple UV-Vis-NIR wavelength excitation spectra (b) of the synthetic ruby SR 2.

The multiple UV-Vis-NIR wavelength excitation spectra of the synthetic ruby samples showed that the Be-heated synthetic ruby samples were different from the unheated and traditionally heated samples. The presence of the 475 nm peak from the Be-heated samples was the distinctive absorption peak observed in the visible region. To confirm the observation of this peak, the spectra were compared after data processing, which included normalization and background subtraction. Figure 5 shows a set of a couple of the compared

samples. It was confirmed that the peak at 475 nm was only found for the Be-heated samples. Therefore, it was proposed that this peak (475 nm) arose from a donor state of Be^{2+} in the corundum structure. The intensity in the vicinity of 700 nm for the samples was less than zero, owing to the Cr^{3+} fluorescence signal in ruby. Hence, the excitation spectra were analyzed between 275 and 600 nm.

The a^* and b^* of CIELAB color indices in Fig. 6a were obtained for the unheated, traditionally heated, and Be-heated synthetic ruby samples. The Be-heated samples showed an increase of the yellow content ($+b^*$) and a decrease of the red content ($+a^*$). This was the reason for the appearance of the orange color. The values of brightness (L^*) in Fig. 6b exhibited no relationship to the heating condition.

The UV fluorescence properties of the synthetic ruby samples were observed in the shortwave (SW) and longwave (LW) regions, as shown in Table 3. According to the results, the unheated and traditionally heated samples showed similar strong fluorescence in the SW and LW regions, whereas the Be-heated samples exhibited weak to inert fluorescence in the SW region and moderate to weak fluorescence in the LW region.

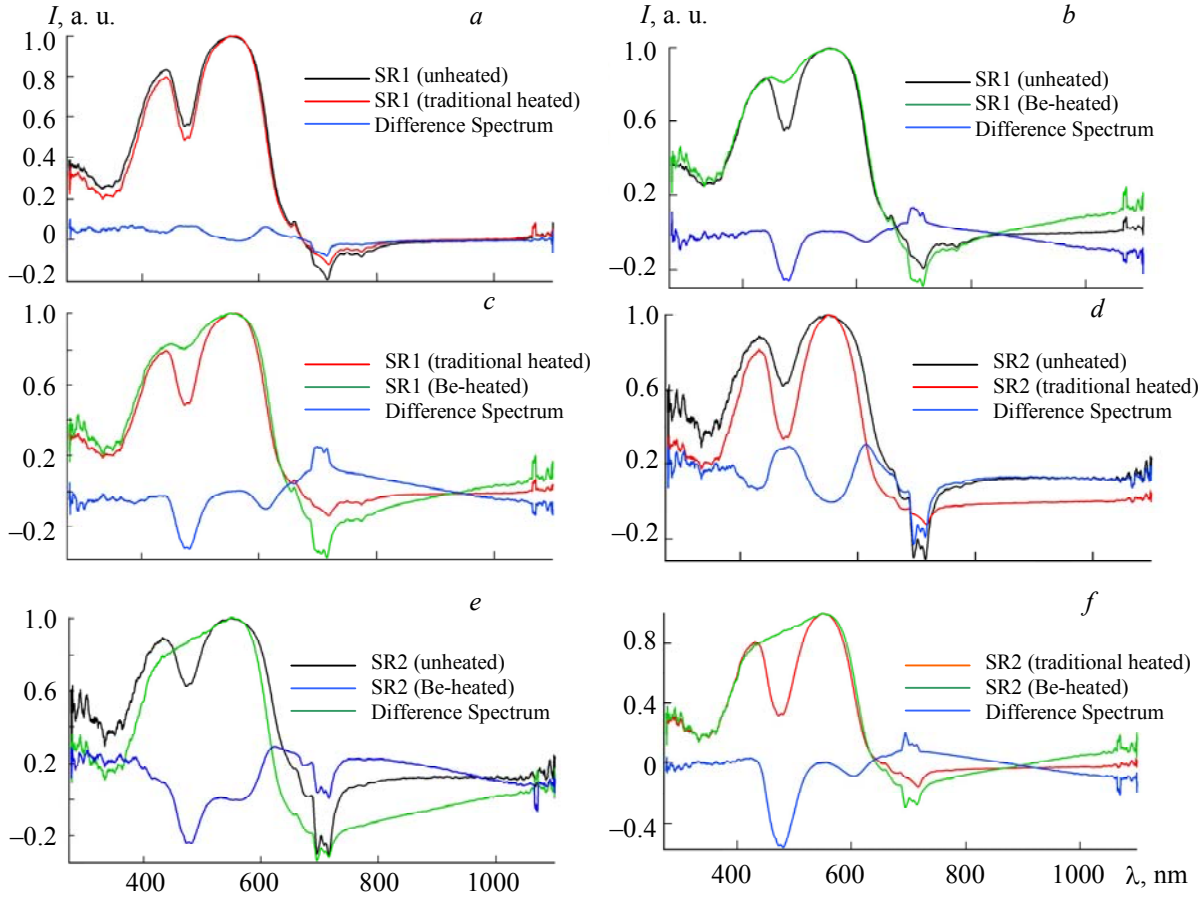

Fig. 5. Multiple UV-Vis-NIR wavelength excitation spectra of the synthetic ruby samples with normalization and background subtraction.

TABLE 3. UV Fluorescence Properties of the Synthetic Ruby Samples

Sample	UV fluorescence	
	SW	LW
SR 1 (unheated)	Strong	Strong
SR 1 (traditionally heated)	Strong	Strong
SR 1 (Be-heated)	Weak to inert	Moderate to weak
SR 2 (unheated)	Strong	Strong
SR 2 (traditionally heated)	Strong	Strong
SR 2 (Be-heated)	Weak to Inert	Moderate to weak

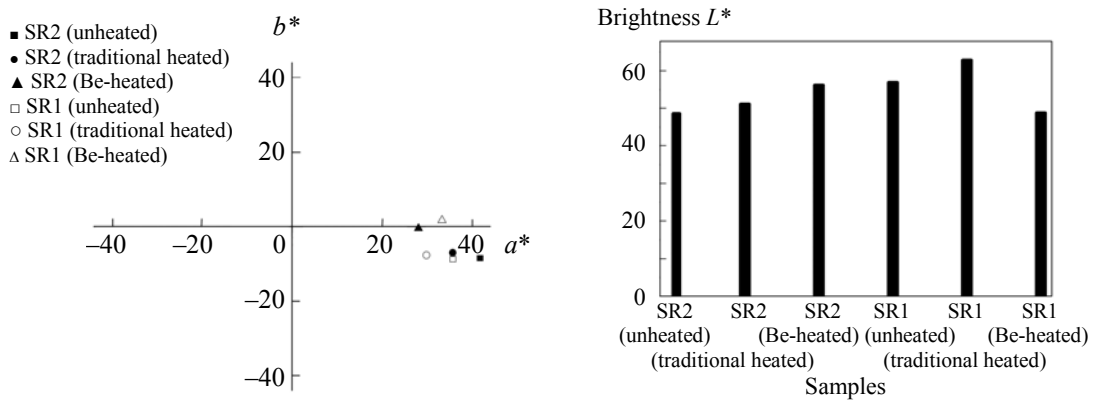

Fig. 6. a^*, b^*, and L^* of CIELAB color indices of the synthetic ruby samples.

The causes of the orange color in the Be-treated synthetic ruby samples were described by the color center from energy band theory. Pure α-Al_2O_3 was colorless owing to its energy band gap of 8.8 eV. For the unheated as well as the traditionally heated synthetic ruby samples, the red color was caused by the Cr^{3+} states at 3.06, 2.23, and 1.79 eV, which corresponded to 405, 555, and 693 nm. These states were stably located in the energy band gap, as shown in Fig. 7a. Furthermore, the yellow color in the Be-treated synthetic ruby samples was caused by Be^{2+} donor state color centers located at 2.61 eV, which corresponded to the 475 nm band in the multiple UV-Vis-NIR wavelength excitation spectrum. Thus, the yellow coloration in the synthetic ruby samples affected by Be treatment is effectively caused by the electron transition from the Be^{2+} donor state to the conduction band, shown in Fig. 7b. After the donating process, the Be^{2+} will be changed to Be^{3+}. Moreover, the fluorescence intensity of the Be-treated synthetic ruby samples decreases owing to the Be^{2+} donor state at 2.61 eV, as shown in Fig. 7c.

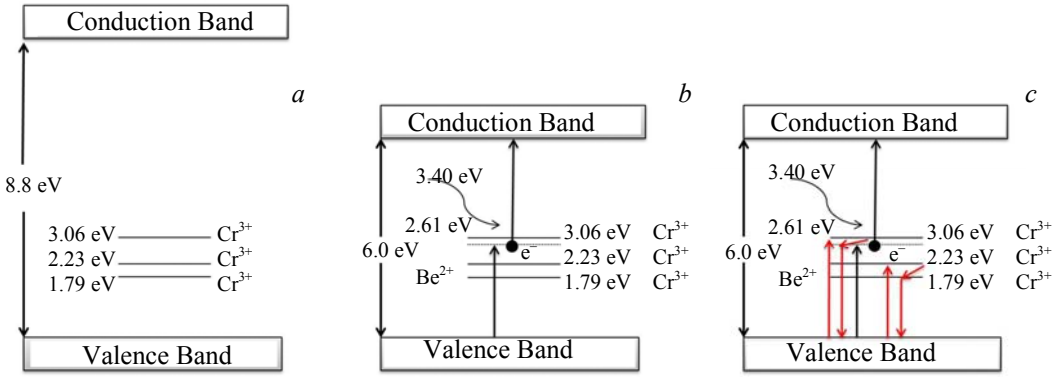

Fig. 7. Energy band model of Cr^{3+} states in (a) unheated and traditionally heated synthetic rubies and (b) the Be^{2+}donor state in Be-treated synthetic ruby sample, and (c) decrease of fluorescence characteristics (shown as red arrow) in the Be-treated synthetic sample arising from the Be^{2+} donor state.

Conclusion. The spreading of Be atoms was observed in synthetic ruby samples after heating with Be, as detected by LA-ICP-MS. The Be atoms were not located in the Cr environment, which was proved by the Cr *K*-edge XANES spectra that showed similar Cr^{3+} compared with the synthetic unheated and traditionally heated ruby samples. The UV-Vis-NIR absorption spectra could not be distinguished among the synthetic unheated, traditionally heated, and Be-heated ruby samples. The Be-heated synthetic ruby samples turned orange, which was detected by the CIELAB indices as well as the weakening of the UV fluorescence properties. Therefore, the orange coloration was produced by the red color of ruby and the brown-color center of the Be^{2+} donor state detected in the multiple UV-Vis-NIR wavelength excitation spectra at 475 nm.

Acknowledgment. The authors thank the Department of Earth Sciences as well as Department of Physics, Faculty of Science and the Center for Advanced Studies in Industrial Technology of Kasetsart University for preparing the synthetic ruby samples and performing the spectroscopy experiments; the Synchrotron

Light Research Institute (Public Organization) for providing the XAS beam time; and the Gem and Jewelry Institute (Public Organization) for support with the chemical analysis.

We thank Edanz Group (www.edanzediting.com/ac) for editing a draft of this manuscript.

REFERENCES

1. E. Fritsch, G. R. Rossman, *Gems Gemol.*, **23**, No. 3, 126–139 (1987).
2. E. Fritsch, G. R. Rossman, *Gems Gemol.*, **24**, No. 1, 3–15 (1988).
3. E. Fritsch, G. R. Rossman, *Gems Gemol.*, **24**, No. 2, 81–102 (1988).
4. J. L. Emmett, K. Scarratt, S.F. McClure, T. Moses, T. R. Douthit, R. W. Hughes, S. Novak, J. E. Shigley, W. Wang, O. Bordelon, R. E. Kane, *Gems Gemol.*, **39**, No. 2, 84–135 (2003).
5. T. Häger, *Proc. Int. Workshop on Material Characterization by Solid State Spectroscopy: The Minerals of Vietnam*, 24–37 (2001).
6. S. F. McClure, T. Moses, W. Wang, M. Hall, J. I. Koivula, *Gems Gemol.*, **38**, 86–90 (2002).
7. A. Peretti, D. Gunther, *Contributions to Gemlogy*, **1**, 1–48 (2002).
8. K. Schmetzer, D. Schwarz, *J. Gemmol.*, **29**, No. 3, 149–182 (2004).
9. P. Limsuwan, S. Meejoo, A. Somdee, K. Thamaphat, T. Kittiauchawal, A. Siripinyanond, J. Krzystck, *Chin. Phys. Lett.*, **25**, No. 6, 1976–1979 (2008).
10. V. Pisutha-Arnond, T. Häger, P. Wathanakul, W. Atichat, *J. Gemmol.*, **29**, No. 2, 77–103 (2004).
11. V. Pisutha-Arnond, T. Häger, W. Atichat, P. Wathanakul, *J. Gemmol.*, **30**, No. 3-4, 131–143 (2006).
12. P. Wathanakul, T. Häger, W. Atichat, V. Pisutha-Arnond, T. Win, P. Lomthong, B. Sriprasert, C. Sutthirat, *Gems Gemol.*, **42**, No. 3, 87 (2006).
13. P. Wongrawang, N. Monarumit, N. Thammajak, P. Wathanakul, W. Wongkokua, *Mater. Res. Exp.*, **3**, No. 2, 026201 (2016).
14. N. Monarumit, W. Wongkokua, P. Wathanakul, *Proc. 3rd Int. Gem and Jewelry Conf.*, 175–178 (2012).
15. V. Pisutha-Arnond, C. Rochd, W. Atichat, P. Wathanakul, N. Narudeesombat, *Proc. 34th Int. Gemmological Conf.*, 65–68 (2015).
16. R. W. Hughes, *Ruby & Sapphire*, RWH Publishing, USA (1997).
17. V. Sivaprakasam, A. L. Huston, C. Scotto, J. D. Eversole, *Opt. Express*, **12**, No. 19, 4457 (2004).
18. P. Wathanakul, W. Wongkokua, S. Pongkrapan, *Abstr. 19th Annual V. M. Goldschmidt Conf.*, A1421 (2009).
19. P. Songsiriritthigul, W. Pairsuwan, T. Ishii, A. Kakizaki, *Nucl. Instrum. Methods B*, **199**, 565–568 (2003).
20. M. Newville, *J. Synchrotron. Radiat.*, **8**, 322–324 (2001).